The influence of classical resonances on quantum energy levels

B. Ramachandran
Department of Chemistry, Louisiana Tech University, Ruston, Louisiana 71272

Kenneth G. Kay
Department of Chemistry, Bar-Ilan University, Ramat-Gan, Israel 52900

(Received 26 January 1993; accepted 25 May 1993)

In this paper, we examine the behavior of the quantum energy levels of a coupled oscillator system as the zero-order frequencies are varied to carry the corresponding classical system through a resonance. We find that the levels exhibit a pattern that is characteristic of the resonance. This pattern consists of clusters of levels, each containing a number of curves that run roughly parallel to one another and a number of curves that undergo pairwise narrowly avoided crossings. Adiabatic switching calculations show that the "parallel" curves are associated with states within the classical resonance region, while the narrowly avoiding curves are associated with states that are outside this region. It is further shown that the curves describing resonance states are formed from zero-order nonresonant curves by the overlap of many avoided crossings. This reorganization of multiply intersecting lines into parallel curves reflects the classical reorganization of phase space at a resonance.

I. INTRODUCTION

Nonlinear resonances are of central importance in classical mechanics. The presence of even a single resonance can profoundly affect the dynamics of energy transfer between coupled subsystems.[1–6] The existence of more than one resonance may lead to the destruction of Kolomogorov–Arnold–Moser (KAM) surfaces and nonintegrability.[7,8] The crucial role of nonlinear resonances in the formation of dynamic instabilities is clearly expressed in Chirikov's[7] criterion for the onset of chaos, which requires the overlap of neighboring resonances.

As one might expect from correspondence principle arguments, nonlinear resonances are also of great importance in determining the behavior of quantum systems. The influence of resonances on the dynamics and spectroscopy of such systems has been investigated by many workers.[9–24] In this paper, we examine how nonlinear resonances affect the pattern of energy levels of a quantum system when a parameter in the Hamiltonian is varied.

A number of workers have investigated the influence of resonances on the energy levels of systems with fixed Hamiltonians.[9–14,17–19,25] There has also been much discussion of the effect of these resonances on the pattern of energy levels that result when a parameter in the Hamiltonian is varied.[20–23,26–29] It has been proposed that the isolated avoided crossing of a pair of levels constitutes the quantum analog of a resonance.[20–22] It has been further conjectured that multiple overlapping avoided crossings constitute the analog of overlapping resonances and thus represent a signature of classical chaos in a quantum system.[20–22,30] Avoided crossings associated with overlapping resonances have been cited as the source of Gaussian orthogonal ensemble (GOE) level statistics in chaotic quantum systems.[26,31,32] In addition, a number of other statistical properties of avoided crossings have been linked to the chaotic properties of the corresponding classical system.[33–36]

The reasons for associating avoided crossings with classical resonances can be formulated in a number of ways[20,22(b),26] but these are equivalent to the following argument:[22(b),26] focusing on a system of two degrees of freedom for simplicity, we note that intersection of a pair of levels implies semiclassically that $H(J_1,J_2) = H(J_1',J_2')$, where J_i and J_i' are action variables for the two states. If $|J_i - J_i'|$ is small, we may expand $H(J_1',J_2')$ about $J_i' = J_i$ to obtain

$$H(J_1',J_2') = H(J_1,J_2) + (J_1 - J_1')\omega_1 + (J_2 - J_2')\omega_2 + \cdots, \tag{1}$$

where $\omega_i = \partial H/\partial J_i$ are the frequencies associated with the actions J_i. Now, substituting the semiclassical quantization condition $J_i = (n + \alpha_i/4)\hbar$, where α_i is the Maslov index, we obtain

$$(n_1 - n_1')\omega_1 = (n_2' - n_2)\omega_2 \tag{2}$$

at the crossing, which is equivalent to the classical resonance condition $n\omega_1 = m\omega_2$. Thus, the intersection of two levels in a quantum system appears to imply the existence of a resonance in the corresponding classical system. The intersection described above becomes an avoided crossing when coupling between the states lifts the degeneracy, as in the textbook two-level problem.[37]

Although this argument seems compelling, it has been apparent for some time that the relationship between resonances and avoided crossings cannot be quite so simple. If this relationship were correct, one would expect that the mixing of wave functions near an isolated avoided crossing would correspond to the classical rearrangement of phase space near a resonance which leads to formation of resonant tori; the splitting between levels at an avoided crossing should then be related to a classical frequency for resonant motion. However, it has been shown repeatedly that the mixing of the wave functions in an isolated avoided crossing does not correspond to any classical process, but is a consequence of tunneling[12,17,23,27,28,38–43] between tori associated with the nearly intersecting levels (see, however,

Ref. 44). Thus, the energy difference between the repelling levels is not related to a classical frequency, but vanishes faster than any power of $\hbar$ in the classical limit. Ozorio de Almeida[23] has, in fact, shown that the states that are involved in this tunneling do not even lie within the resonance, but correspond to nonresonant tori.

These considerations raise a number of questions concerning the relationship between isolated resonances and avoided crossings. (1) How do the energy levels of a quantum system behave when a parameter change carries the corresponding classical system through a resonance? If it is true that avoided crossings do not directly signify a resonance, what does? Is there, in fact, any characteristic pattern in a plot of levels vs a parameter that is indicative of a resonance? (2) How is the specifically classical nature of resonance formation reflected in such a plot? Can this classical effect be distinguished from nonclassical effects? (3) If the above argument concerning the relationship between resonances and avoided crossings is not entirely correct, why? How can it be corrected? The goal of this paper is to investigate these issues using a simple two-dimensional system as an example.

The remainder of this paper is based on the following plan: In Sec. II, we describe the low-energy classical dynamics of the system we choose to study and examine its behavior near a strong resonance. In Sec. III, we describe the behavior of the quantum energy levels plotted as a function of a Hamiltonian parameter in the vicinity of this resonance. We also relate this behavior to the classical resonance by studying closely related model resonance Hamiltonians, obtained by simplifying the nature of the coupling in the original Hamiltonian. In Sec. IV, we verify the conclusions of Sec. III by analyzing the quantizing trajectories of the fully coupled system. Finally, in Sec. V we present a discussion and summary of the main results.

II. PRELIMINARIES

We examine a simple, two-dimensional system consisting of a Morse oscillator coupled to a harmonic oscillator. The system is described by the Hamiltonian

$$H=\tfrac{1}{2}(p_x^2+p_y^2+\omega_2^2y^2)+\rho p_x p_y+D(1-e^{-\beta x})^2, \tag{3}$$

where the harmonic frequency ω_2 is varied to take the system into and out of resonances. The remaining parameters are chosen to be $D=10.0$, $\rho=0.10$, and $\beta=(2D)^{-1/2}$. With this choice for β, the low-energy harmonic frequency of the Morse oscillator $\Omega=(2D\beta^2)^{1/2}$ has the value 1.0.

In Fig. 1, we show the Poincare surface of section for a few typical low energy trajectories of this system with $\omega_2=0.80$. Two major types of trajectories can be clearly identified—trajectories that belong to the 1:1 resonance, and nonresonant trajectories. There are two types of nonresonant trajectories—those confined to the "lagoon" formed by the separatrix, and those that envelope the separatrix. The relative volumes of phase space occupied by these two types of nonresonant trajectories depend on the value of ω_2. As has been shown for a similar case, trajectories belonging to the 1:1 resonance resemble those for a system with uncoupled normal modes, while nonresonant trajectories resemble those for a system with uncoupled local modes.[13,45]

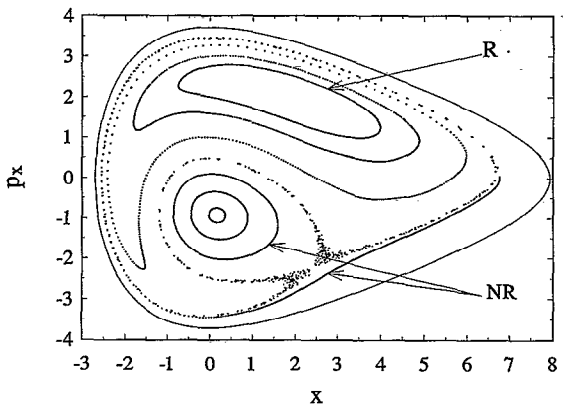

FIG. 1. A Poincaré surface of section for a few typical trajectories of the Hamiltonian of Eq. (3) at $\omega_2=0.80$. A typical resonant trajectory is labeled "*R*", while two types of nonresonant trajectories are labeled "*NR*." The mildly chaotic trajectory lies on the separatrix between the resonant and nonresonant regions of phase space. The nonresonant trajectory that has dense intersections along the lower portion of the figure also has several intersections on the upper portion, but these lie very close to those of the separatrix trajectory.

The behavior of the system in the vicinity of a resonance can be analyzed by the well-known procedure of Chirikov.[7] We express the Hamiltonian of Eq. (3) in terms of actions and angles appropriate for the uncoupled ($\rho=0$) system

$$H(\mathbf{p},\mathbf{q})=H_0(J_1,J_2)+\rho p_1(J_1,\theta_1)p_2(J_2,\theta_2), \tag{4}$$

where

$$H_0(J_1,J_2)=\Omega\left(1-\frac{J_1\Omega}{4D}\right)J_1+\omega_2 J_2, \tag{5}$$

is a function only of the Morse and harmonic actions (J_1,J_2). The Morse oscillator momentum is explicitly given by the expression[46,47]

$$p_1(J_1,\theta_1)=(2D)^{1/2}\frac{\omega_1}{\Omega}\lambda\sin\theta_1(1-\lambda\cos\theta_1)^{-1}, \tag{6}$$

where the action (energy) dependent Morse frequency ω_1 is given by

$$\omega_1(J_1)=\left(1-\frac{J_1\Omega}{2D}\right)\Omega \tag{7}$$

and

$$\lambda=\left(1-\frac{\omega_1^2}{\Omega^2}\right)^{1/2}. \tag{8}$$

The harmonic oscillator momentum is expressed as

$$p_2(J_2,\theta_2)=(2\omega_2 J_2)^{1/2}\sin\theta_2. \tag{9}$$

Expanding Eq. (6) in a Fourier series, substituting the result in Eq. (4), and simplifying, we obtain

$$H=H_0(J_1,J_2)-2\rho(D\omega_2 J_2)^{1/2}\frac{\omega_1}{\Omega}\sum_{n=1}^{\infty}\left[\frac{1-(\omega_1/\Omega)}{1+(\omega_1/\Omega)}\right]^{n/2}$$
$$\times(-1)^n\cos(n\theta_1-\theta_2). \tag{10}$$

Most of the interaction terms in Eq. (10) vary rapidly with time and give negligible contributions. Near an n:1 resonance, however, where the condition $n\omega_1-\omega_2=0$ is approximately obeyed, the term involving $\cos(n\theta_1-\theta_2)$ varies slowly and may dominate the sum. Thus, retaining only the term proportional to $\cos(\theta_1-\theta_2)$, one obtains an approximate Hamiltonian which describes the system's behavior in the vicinity of the 1:1 resonance

$$H=H_0(J_1,J_2)+2V(J_1,J_2)\cos(\theta_1-\theta_2), \tag{11}$$

where

$$V(J_1,J_2)=\rho(D\omega_2 J_2)^{1/2}\frac{\omega_1}{\Omega}\left[\frac{1-(\omega_1/\Omega)}{1+(\omega_1/\Omega)}\right]^{1/2}. \tag{12}$$

For further analysis, it is advantageous to subject the expression of Eq. (11) to a canonical transformation using a generating function of the type $F_2(\theta_1,\theta_2,I_1,I_2)$, where (I_1,I_2) are the new actions conjugate to the new angles (ϕ_1,ϕ_2). Choosing

$$F_2=\tfrac{1}{2}[(\theta_1+\theta_2)I_1+(\theta_1-\theta_2)I_2]$$

yields $J_1=(I_1+I_2)/2$, $J_2=(I_1-I_2)/2$, $\phi_1=(\theta_1+\theta_2)/2$, and $\phi_2=(\theta_1-\theta_2)/2$. Expressing the Hamiltonian in terms of the new variables and approximating the coupling factor $V(J_1,J_2)$ by a constant V_R, we obtain the resonant Hamiltonian of Chirikov[7]

$$H(I_1;I_2,\phi_2)=\tfrac{1}{2}[\omega_1' I_1^2+(\Omega+\omega_2)I_1]+H_R, \tag{13}$$

where

$$H_R=\tfrac{1}{2}[\omega_1' I_2^2+(\omega_1-\omega_2)I_2]+2V_R\cos(2\phi_2), \tag{14a}$$

$$=\tfrac{1}{2}\omega_1'[I_2+(\omega_1-\omega_2)/2\omega_1']^2+2V_R\cos(2\phi_2)-E' \tag{14b}$$

and $\omega_1=(1-I_1\Omega/4D)\Omega$, $\omega_1'=-\Omega^2/8D$, and $E'=(\omega_1-\omega_2)^2/8\omega_1'$.

Note that since ϕ_1 does not appear in this Hamiltonian, I_1 is a constant of motion. The term H_R is the Hamiltonian for a one-dimensional hindered rotor with angular momentum $I_2+(\omega_1-\omega_2)/2\omega_1'$ and angle coordinate ϕ_2. Since the "mass" $1/\omega_1'$ of the rotor is negative, we may think of the motion as taking place in the inverted potential $-2V_R\cos(2\phi_2)$. This system has two characteristic types of trajectories—librating orbits with energies within the cosine barrier $2V_R>H_R+E'>-2V_R$ and rotating orbits with energies beyond the barrier $H_R+E'<-2V_R$. The librating orbits correspond to resonant trajectories of the original system, while the rotating orbits correspond to nonresonant trajectories of the original system. The trajectory with $H_R+E'=-2V_R$ serves as a separatrix dividing phase space into the resonant and nonresonant regions. In Sec. III, we shall return to this Hamiltonian and analyze its quantum behavior.

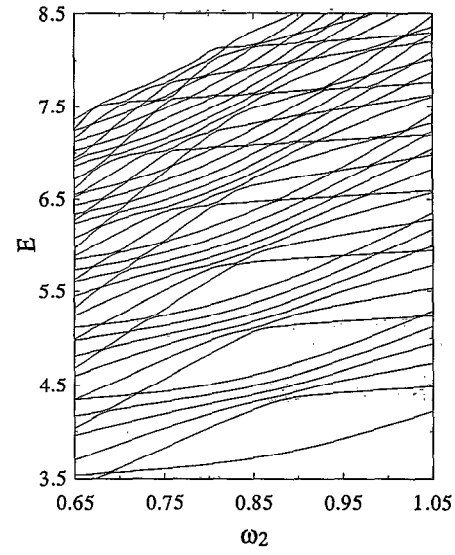

FIG. 2. Several quantum energy levels of the Hamiltonian of Eq. (3) as a function of the harmonic frequency ω_2.

III. QUANTUM ENERGY LEVEL CURVES

The quantum energy levels of our system are obtained by diagonalizing the Hamiltonian of Eq. (3) in a direct product basis of the energy eigenfunctions of the Morse and harmonic oscillators $[\zeta_{n_1,n_2}(x,y)]=[\psi_{n_1}(x)\otimes\varphi_{n_2}(y)]$. The Morse eigenfunctions $\psi_{n_1}(x)$ are obtained by diagonalizing the Morse Hamiltonian in a basis of infinite square well eigenfunctions.

In Fig. 2, we present several energy levels of our system as a function of the harmonic frequency ω_2. The figure consists of a repeated pattern of level clusters. The clusters are especially easy to identify at lower energies. Each cluster consists of a few almost parallel curves at high energy and a few curves that undergo isolated crossings with each other at lower energies. The number of levels in the clusters increases with increasing energy. The avoided crossings near the lower and upper ranges of ω_2 plotted in Fig. 2 result from the overlapping of different clusters.

Each cluster is associated with the resonance. In particular, the clusters are equivalent to the energy level "polyads"[14] identified in previous studies of resonant systems with fixed Hamiltonians.[11,13,14,17–19,25] This can be shown as follows: A close approximation to the energy level curves of a given cluster can be obtained by diagonalizing the Hamiltonian in a small, restricted basis, consisting only of the $(n+1)$ zero-order states for which $n_1+n_2=n$, where n is a fixed value that identifies the cluster. The matrix elements of H are thus given by

$$H_{m_1m_2,n_1n_2}$$
$$=(E^0_{m_1,m_2}\delta_{m_1,n_1}+V_{m_1m_2,n_1n_2})\delta_{m_1+m_2,n}\delta_{n_1+n_2,n}, \tag{15}$$

where

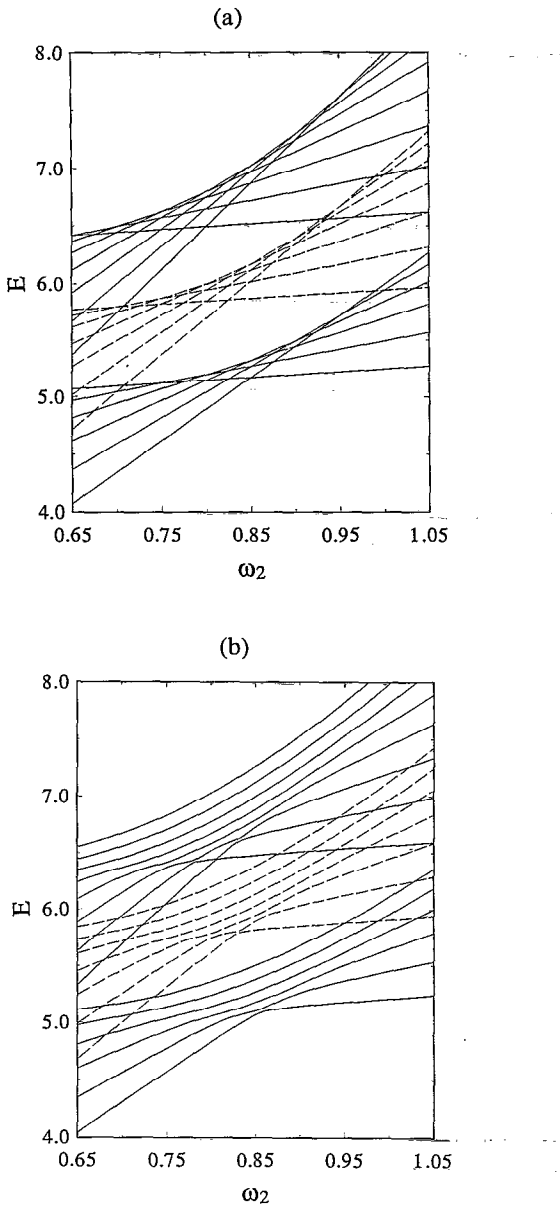

FIG. 3. (a) Zero-order energy levels of the system corresponding to $n_1+n_2=n=5$, 6, and 7 plotted as a function of the harmonic frequency ω_2; (b) the energy levels of the system resulting from diagonalizing the Hamiltonian of Eq. (3) in a basis restricted to those functions satisfying $n_1+n_2=n$ for $n=5$, 6, or 7. In both figures, the levels corresponding to $n=5$ and 7 are plotted using solid lines, while the $n=6$ levels are shown as dashed lines.

$$E^0_{m_1m_2}=\left(m_1+\frac{1}{2}\right)\hbar\Omega-\left(m_1+\frac{1}{2}\right)^2\frac{\hbar^2\Omega^2}{4D}+\left(m_2+\frac{1}{2}\right)\hbar\omega_2 \tag{16}$$

is the energy of the uncoupled Morse-harmonic system and

$$V_{m_1m_2,n_1n_2}=\rho\langle\xi_{m_1m_2}|p_xp_y|\xi_{n_1n_2}\rangle \tag{17}$$

is the coupling.

For convenience, we restrict our attention to clusters with $n=5$, 6, and 7. The zero-order energies $E^0_{m_1m_2}$ for these clusters are shown in Fig. 3(a) and the energy levels resulting from diagonalizing H in the restricted basis are shown in Fig. 3(b). As implied by Eq. (16), the zero-order energies of Fig. 3(a) form a web of intersecting straight lines when plotted as a function of ω_2. On the other hand, the energy levels in Fig. 3(b) are in qualitative and quantitative agreement with the accurate energy levels of Fig. 2. Since the restricted basis does not take into account the coupling between levels belonging to different clusters, the levels belonging to different clusters in Fig. 3(b) undergo true crossings. We note that while the parallel curves in the clusters do not appear to undergo avoided crossings with one another in Fig. 3(b), their formation can be viewed as the result of strongly overlapping multiple avoided crossings of the unperturbed levels of Fig. 3(a).

Let us now reexpress the matrix elements appearing in Eq. (15) in terms of the quantum numbers $n=n_1+n_2$ and $m=n_1-n_2$. Then, recognizing that the interaction $V_{m_1m_2,n_1n_2}$ couples only harmonic states with $n_2=n_1\pm1$, Eq. (15) is found to have the form

$$H_{mn,m'n'}=\left\{\tfrac{1}{2}[(n+1)^2\hbar^2\omega_1'+(n+1)\hbar(\Omega+\omega_2)]\times\frac{\hbar^2\omega_1'}{2}m^2+\frac{\hbar}{2}(\omega_1-\omega_2)m\right\}\delta_{mm'}\delta_{nn'}+V_{mn,m'n'}(\delta_{m,m'+2}+\delta_{m,m'-2})\delta_{nn'}, \tag{18}$$

where the frequency ω_1 depends on the quantum number n as

$$\omega_1=\Omega\left[1-\frac{(n+1)\hbar\Omega}{4D}\right].$$

This expression makes it clear why the number of levels in the clusters increases with energy. The first two terms in Eq. (18) describe an increasing function of n (for physically meaningful values of this quantum number) and establish the energy "origin" of the cluster. The number of levels in such a cluster is $n+1$ since diagonalization of the Hamiltonian is carried out in the basis of the $n+1$ functions with $m=-n,\ -n+2,\ldots,n$. A comparison of this analysis to that of Ref. 14 also establishes the equivalence of the clusters to energy level polyads.

The relationship of the clusters to the classical resonance can be established by quantizing the classical resonance Hamiltonian of Eq. (13). For this, we replace the momenta I_j by operators $-i\hbar\partial/\partial\phi_j$. It then becomes clear that matrix elements of this operator in the basis of free rotor eigenstates $R_{nm}=B\exp[i(n+1)\phi_1+im\phi_2]$ are identical to the matrix elements given by Eq. (18), provided that $V_{mn,m'n'}$ are approximated as the constant V_R for all coupled states. Thus our diagonalization of the quantum Hamiltonian of Eq. (18) is seen to be "almost" equivalent to solution of the Schrödinger equation associated with the resonance Hamiltonian of Eq. (13). We now show that the resonance Hamiltonian yields energy level curves that are qualitatively similar to those of the exact Hamiltonian. The nature of these curves can be directly correlated with the resonant/nonresonant property of the levels, as shown below.

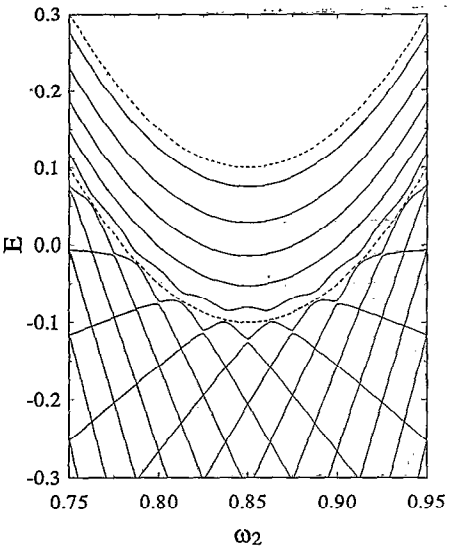

FIG. 4. Several energy levels of the hindered rotor Hamiltonian of Eqs. (14) as a function of the frequency ω_2. The parameters used are $V_R=0.05$, $\omega_1=0.85$, and $D=10$. The dashed curves indicate the values $2V_R-E'$ and $-2V_R-E'$, which are the boundaries of the resonance. Note that the energy levels in the region enclosed by the dashed curves run nearly parallel to each other, while those outside this region show isolated avoided crossings.

In Fig. 4, we show the energy levels obtained by numerically diagonalizing the resonance Hamiltonian operator corresponding to H_R of Eq. (14) in a large basis of free rotor functions. The qualitative similarity between this pattern and a cluster in Fig. 3(b)—a finite number of "parallel" curves, and curves that display pairwise avoided crossings—is immediately apparent. The most obvious difference between the two sets of curves, viz., the finite extent of the clusters of Fig. 3(b) vs the infinite (in principle) extent of the pattern in Fig. 4, is due to the fact that our diagonalization in Fig. 3(b) is performed in the finite basis of $n+1$ functions, while the formally exact diagonalization of the resonance Hamiltonian would require an infinite basis.

We note that the parallel energy level curves shown in Fig. 4 are confined to energies $2V_R > E+E' > -2V_R$ that lie within the cosine potential of the resonance Hamiltonian; these levels are associated with states that lie within the resonance. The other energy levels, which undergo sharp avoided crossings, have energies $E+E' < -2V_R$; such levels are associated with states that lie outside the resonance. This behavior of the energy levels for states lying within and outside a resonance zone can be shown to apply for general values of the parameters in H_R and can be given an analytical explanation, as demonstrated in the Appendix.

IV. SEMICLASSICAL ASSIGNMENT OF STATES

In the preceding section, we examined the structure of a cluster and showed that the levels running parallel to each other are associated with states inside a resonance, while those undergoing avoided crossings are associated with states outside a resonance. These conclusions were, however, obtained for a model Hamiltonian derived from the Hamiltonian of Eq. (3) by applying a sequence of simplifying assumptions concerning the interactions between the states. In view of these approximations and the resulting differences between Figs. 2 and 4, it is highly desirable to verify our conclusions for the original system by a direct and independent procedure.

We thus seek a way of classifying the states associated with the levels of Fig. 2 as resonant or nonresonant without resorting to the assumptions of the previous section. To accomplish this, we generate the quantizing classical tori associated with these states and determine whether they are located within the classical 1:1 resonance region. For alternative methods of assigning the states in a resonance zone, see Refs. 14(b), 48, and 49.

We generate the quantizing tori of the present system by applying the method of adiabatic switching.[29,39,50–56] The method is based on writing the Hamiltonian of the fully coupled system $H(\mathbf{p},\mathbf{q})$ as

$$H(\mathbf{p},\mathbf{q})=H_0(\mathbf{p},\mathbf{q})+s(t)H'(\mathbf{p},\mathbf{q}),$$

where H_0 is rigorously integrable and can be quantized by the application of the Einstein–Brillouin–Keller (EBK) rules, H' is a nonseparable perturbation that renders H nonintegrable, and $s(t)$ is a switching function that "turns on" the perturbation over a time interval $0 \leqslant t \leqslant T$. Provided that H_0 is chosen appropriately, and T is a sufficiently long interval, the quantized actions are expected to be adiabatically conserved during the switching process, thus yielding the quantized energy levels of the coupled system at the end of the switching. The spread in the final energies of an ensemble of trajectories, as reflected in the magnitude of the root-mean-square deviation $\Delta E_{\rm rms}$, provides a measure of the accuracy of the fundamental assumption in the adiabatic switching (AS) method, viz., the adiabatic conservation of actions. We refer the reader to Ref. 55 for details concerning the implementation of this method.

In the case of the present system, it is clear from Fig. 1 that there are two main types of trajectories in the vicinity of the 1:1 resonance, viz., the nonresonant, local mode trajectories and the resonant, normal mode trajectories. Thus, to generate quantizing trajectories that lie outside the resonance, we apply the AS procedure with a zero-order Hamiltonian that describes independent local modes given by[51]

$$H_0=\tfrac{1}{2}(p_x^2+p_y^2+\omega_2^2y^2)+D(1-e^{-\beta x})^2 \tag{19a}$$

and turn on the perturbation as

$$H'(t)=s(t)\rho p_x p_y. \tag{19b}$$

To generate resonant quantizing trajectories, we apply the AS method with a zero-order Hamiltonian that is quadratic in momenta and coordinates

$$H_0=\tfrac{1}{2}(p_x^2+p_y^2+2\rho p_x p_y+\Omega^2x^2+\omega_2^2y^2), \tag{20a}$$

which admits a description of the oscillators as two independent normal modes, and turn the perturbation on as

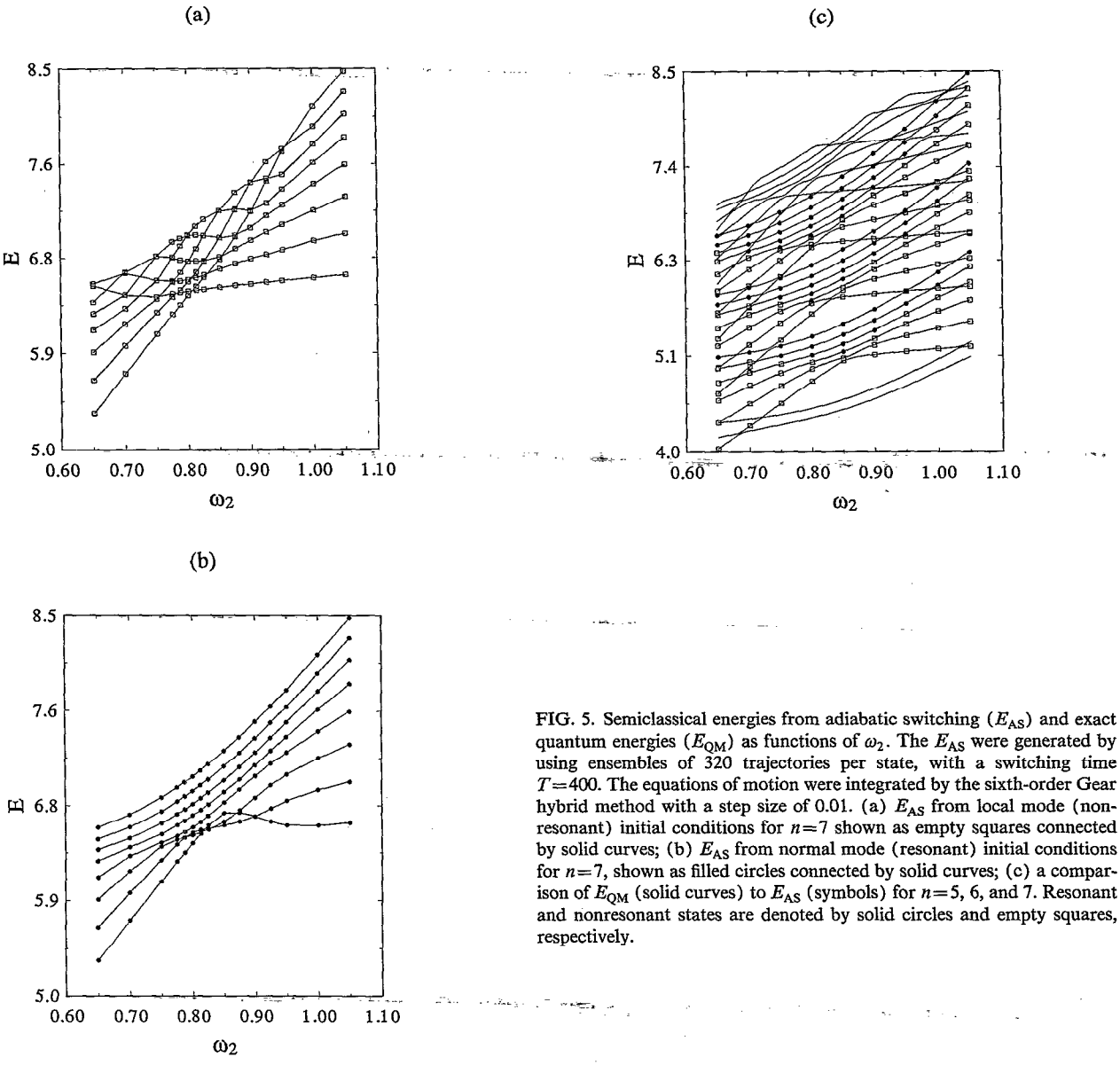

FIG. 5. Semiclassical energies from adiabatic switching (E_{AS}) and exact quantum energies (E_{QM}) as functions of ω_2. The E_{AS} were generated by using ensembles of 320 trajectories per state, with a switching time $T=400$. The equations of motion were integrated by the sixth-order Gear hybrid method with a step size of 0.01. (a) E_{AS} from local mode (nonresonant) initial conditions for $n=7$ shown as empty squares connected by solid curves; (b) E_{AS} from normal mode (resonant) initial conditions for $n=7$, shown as filled circles connected by solid curves; (c) a comparison of E_{QM} (solid curves) to E_{AS} (symbols) for $n=5$, 6, and 7. Resonant and nonresonant states are denoted by solid circles and empty squares, respectively.

$$H'(t)=s(t)[D(1-e^{-\beta x})^2-\tfrac{1}{2}\Omega^2x^2]. \quad (20b)$$

The semiclassical energy levels E_{AS} for the cluster with $n=7$ resulting from local mode (nonresonant) initial conditions are plotted as a function of ω_2 in Fig. 5(a). The crossing of the energy levels seen in this figure are indeed genuine crossings, as verified by the observed switch in the relative energies of states as they pass through a crossing. The ΔE_{rms} values of the energy levels (not shown in the figure) are largest for the higher energy states, especially between $\omega_2=0.70$ and 0.90, and smallest for the lower energy states, indicating that the lower energy states are the nonresonant states in the cluster.

The semiclassical energy levels E_{AS} for the cluster with $n=7$ resulting from normal mode (resonant) initial conditions are plotted as a function of ω_2 in Fig. 5(b). The ΔE_{rms} values (not shown in the figure) are largest for the lower energy states, especially between $\omega_2=0.75$ and 0.90, and smallest for the higher energy states, indicating that the higher energy states are the resonant states in the cluster. In contrast to Fig. 5(a), the resonant energy levels show no crossings in the entire frequency range examined, in keeping with the conclusions of the preceding sections.

It should be noted that, whereas the local mode H_0 does not lead to an accurate AS treatment for normal mode states, the normal mode H_0 does sometimes lead to a successful AS treatment for local mode states. This occurs when the difference between Ω and ω_2 is large enough that the zero-order normal modes of Eq. (20a) resemble local harmonic modes with frequencies Ω and ω_2. Such a normal mode H_0 successfully produces local mode tori for states in which the harmonic oscillator quantum number is high and the Morse oscillator quantum number is low. Thus, accuracy of both the normal and local mode AS treatments in cases of this kind indicates nonresonant be-

havior. This also explains why the lowest lying curves of Fig. 5(b) show nonresonant behavior (crossings) and tend to follow the local mode energy curves of Fig. 5(a) at low and high values of ω_2.

These considerations, together with comparison of the two sets of E_{AS} with the exact quantum energies E_{QM}, now allow us to classify the *quantum* states as resonant or nonresonant. Figure 5(c) presents this assignment and compares the corresponding values of E_{AS} and E_{QM} for clusters $n=5$, 6, and 7. The agreement between the semiclassical and exact quantum energies is seen to be very good.

It is clear from Figs. 5(a) and 5(c) that, despite the good agreement of the selected E_{AS} with E_{QM}, the AS method is unable to reproduce the avoided crossings exhibited by the actual nonresonant levels. This failure is consistent with the interpretation of such level repulsion as a symptom of tunneling. It is well known that primitive semiclassical techniques, such as the AS method, are unable to treat tunneling phenomena.[27,28,57] These results, therefore, confirm our expectations from the previous section and serve to establish that the assumptions made in reducing the Hamiltonian of Eq. (3) to the hindered rotor Hamiltonian of Eq. (A1) of the Appendix do not alter the conclusions drawn therein.

The locations and widths of resonance zones in the energy-parameter plot of Fig. 5(c) can be understood from an examination of the resonance Hamiltonian of Eq. (14b). The zero-order state with quantum number $m=I_2/\hbar$ will lie within the resonance region if its energy, as given by the first term in Eq. (14b), falls within the limits of $(0,4V_R)$. This leads to the condition

$$-\Delta I < m\hbar + \frac{(\omega_2-\omega_1)}{2\omega_1'} < \Delta I, \tag{21}$$

where

$$\Delta I = \left(\frac{8V_R}{|\omega_1'|}\right)^{1/2} \tag{22}$$

is the action space half-width of the resonance.[7] Recalling that the values of m are restricted to $-n$, $-n+2,\ldots,n$, one finds that the number of states in the resonance is

$$[\Delta I/\hbar], \quad \text{if } n\hbar < \Delta I \quad \text{and} \quad |\omega_2-\omega_1| < |2\omega_1'|(n\hbar-\Delta I), \tag{23a}$$

$$n, \quad \text{if } \Delta I > n\hbar \quad \text{and} \quad |\omega_2-\omega_1| < |2\omega_1'|(\Delta I-n\hbar), \tag{23b}$$

$$\left[\frac{1}{2\hbar}(\Delta I+n\hbar-|\omega_2-\omega_1|/|2\omega_1'|)\right], \quad \text{otherwise}, \tag{23c}$$

where the square brackets indicate the integer part. These results show that the number of levels in the resonance is greatest at the frequency

$$\omega_2=\omega_1=\Omega\left[1-\frac{(n+1)\hbar\Omega}{4D}\right], \tag{24}$$

which locates the "centers" of the clusters in Fig. 5. Application of Eqs. (23) and (24) to the clusters labeled by $n=5$, 6, and 7 yields the results presented in Table I. A comparison of these results to the numbers of filled circles at each ω_2 in Fig. 5(c) shows good agreement.

TABLE I. Centers of clusters and number of levels in resonance for each cluster, as determined by Eqs. (27) and (28).

n	ω_2 at center	Range of ω_2[a]	Number of levels in resonance
5	0.85	(0.825–0.875)	4
		(0.775–0.825), (0.875–0.925)	3
		(0.725–0.775), (0.925–0.975)	2
		(0.675–0.725), (0.975–1.025)	1
6	0.825	(0.800–0.850)	5
		(0.750–0.800), (0.850–0.900)	4
		(0.700–0.750), (0.900–0.950)	3
		(0.650–0.700), (0.950–1.000)	2
		(0.600–0.650), (1.000–1.100)	1
7	0.8	(0.725–0.875)	5
		(0.675–0.725), (0.875–0.925)	4
		(0.650–0.675), (0.925–0.975)	3
		(0.600–0.650), (0.975–1.00)	2
		(1.00–1.10)	1

[a]The ranges were obtained by using values of $V_R=1/40$ for $n=5$ and $V_R=5/128$ for $n=6$ and 7. These yield values of $\Delta I=4$, 5, and 5 for $n=5$, 6, and 7, respectively.

V. DISCUSSION AND SUMMARY

We have shown that a distinctive pattern emerges when the energy levels of our system are plotted as a function of a parameter that carries the system through the 1:1 resonance. This pattern, which is characteristic of the resonance, consists of a set of clusters, each of which contains two kinds of levels—nearly parallel curves produced by states within the classical resonance region, and curves exhibiting sharp, narrowly avoided crossings produced by states outside the classical resonance region.

These results and the accompanying analysis place us in a position to understand the relationship between avoided crossings and resonances. In agreement with the line of reasoning described in the Introduction, we find that isolated avoided crossings do accompany resonances. In fact, we find that, in general, several such avoided crossings can be associated with each resonance. However, in contrast to the usual inferences, but in agreement with the analysis of Ozorio de Almeida,[23] we conclude that the specific levels exhibiting such crossings are not associated with states within the classical resonance zone but with states lying beyond the resonance separatrix.

It is instructive to examine why the argument relating avoided crossings to resonances, described in the Introduction, fails. This reasoning indeed establishes that the condition $H(J_1,J_2) = H(J_1',J_2')$ implies the resonance condition $n\omega_1=m\omega_2$. However, even according to the simplest semiclassical theories, this result does not mean that the energy levels associated with a resonance undergo any apparent form of avoided crossings. To understand this conclusion, we must recall that different sets of action-angle variables are needed to describe tori inside and outside a resonance region. The condition $H(J_1,J_2) = H(J_1',J_2')$ describes intersection of energy levels belonging to a reso-

nance only if J_i and J_i' are action variables specifically appropriate for that resonance. One such action, say J_1, will then be analogous to I_1 of Sec. II and will be a constant of motion, while the other action J_2 will describe the hindered rotor. Since $\omega_i = \partial H/\partial J_i$ are now frequencies of angular motion conjugate to the J_i (and not frequencies for the original uncoupled oscillators), the condition $n\omega_1 = m\omega_2$ $(n>0)$ does not describe the formation of the original (primary) resonance, but that of a higher order (secondary) resonance. Such a resonance exists only if additional Fourier components of the interaction are taken into account. Its proper treatment, in any event, necessitates a further redefinition of the actions. The condition $n\omega_1 = m\omega_2$ can refer to the original resonance only for the choice $n=0$. In that case, the equation $H(J_1,J_2) = H(J_1',J_2')$ describes the crossing of levels very near the separatrix, where the hindered rotor frequency ω_2 is close to zero.[20] The resonance condition does not, however, imply any crossing of the majority of levels within the resonance zone.

It is not hard to show how the argument presented in the Introduction may be corrected so as to lead to the observed cluster structure. Let us take J_i and J_i' appearing in the condition $H(J_1,J_2) = H(J_1',J_2')$ to refer to action variables appropriate for the region outside the resonance (e.g., actions of the uncoupled oscillators). Then, as has been well understood, the condition $(n_1 - n_1')\omega_1 = (n_2 - n_2')\omega_2$ is actually obeyed in the vicinity of an $n{:}m$ resonance by *many* nearby pairs of zero-order levels (n_1,n_2), (n_1',n_2') satisfying $(n_1 - n_1') = n$, and $(n_2 - n_2') = m$. Since, however, the ω_i are generally functions of the n_i, the various levels do not all cross at the same point in the energy-parameter plane; instead, different pairs of levels intersect at slightly different points, forming a web of curves similar to that shown in Fig. 3(a). These curves describe zero-order energy levels which do not incorporate the interaction that is responsible for the formation of the classical resonance. Since the upper portion of the web is dense, the effect of this interaction is to mix together simultaneously many levels of this region. This leads to the formation of the parallel curves by a mechanism that can be described as the multiple overlap of avoided crossings. The strong effect of the perturbation in this case reflects the resonant nature of the corresponding classical motion. Since the lower portion of the web is relatively sparse, the effect of the interaction is essentially restricted to mixing the zero-order energy curves in a pairwise fashion in the vicinity of a crossing, thus producing isolated avoided crossings. The weak perturbation of these levels reflects the nonresonant nature of the corresponding classical motion.

It is important to emphasize that, generally speaking, avoided crossings need not be in any way associated with classical resonances or even with classical regions that are near resonances. For example, if the action variables (J_1,J_2) and (J_1',J_2') appropriate for the two intersecting levels are of different kinds, one cannot expand $H(J_1',J_2')$ in terms of (J_1,J_2) as described in the Introduction and no relationship between a crossing and a classical resonance condition exists. This may happen when intersecting levels are associated with different resonance regions or when one level is associated with a nonresonant zone while another is associated with a resonant region. In our system, cases of this sort occur when local mode and normal mode curves belonging to different clusters undergo avoided crossings, as in Fig. 2.

One of the most intriguing aspects of our results concerns the mechanism for formation of the resonant and nonresonant energy curves. Although both kinds of curves are formed by the avoided crossings of zero-order levels (cf. Fig. 3), these curves are qualitatively different; the resonant curves run parallel to each other and do not resemble the zero-order levels, while the nonresonant curves display distinct avoided crossings at zero-order intersections and are otherwise weakly perturbed versions of the zero-order straight lines. From the strictly quantum mechanical viewpoint, the mechanism producing the two types of curves is the same; the distinctions between these curves concern matters of degree, i.e., they result from different spacings between the zero-order levels. From the semiclassical viewpoint, however, the qualitative differences in the curves reflect fundamentally different physical mechanisms for the state mixing that is responsible for the level repulsion. The state mixing which produces the parallel curves from the intersecting lines has direct classical significance; it is the interaction which reorganizes phase space in the vicinity of a resonance creating, e.g., normal mode tori in place of local mode tori. The separation between adjacent parallel curves is related to a classical frequency for motion in the resonance. In contrast, a large body of evidence[12,17,23,27,28,38–43] suggests that the state mixing which produces the isolated avoided crossings has no classical significance; it appears solely to be the consequence of tunneling between states associated with different tori that are external to the resonance. The splitting between the nearly intersecting curves is related to a tunneling frequency.

Consistent with the belief that multiple overlapping avoided crossings correspond to overlapping resonances, it has been conjectured[20–22] that such crossings should produce complicated, "stochastic" wave functions associated with chaotic systems. Figure 3 demonstrates, however, that certain multiple overlapping avoided crossings correspond to isolated resonances. Such resonances produce nonchaotic classical motion and yield wave functions that have simple nodal patterns and that are in no way stochastic. On the other hand, the work of Graffi *et al.*[30] indicates that certain sets of overlapping avoided crossings may, indeed, correspond to overlapping resonances which produce chaotic classical motion and, presumably, yield stochastic wave functions. Taken together, this suggests that multiple overlapping avoided crossings are not specific symptoms of chaos, but may reflect a more general class of processes that persist in the classical limit and result in macroscopic structural changes in phase space.

We conclude with some comments about the generality of the results presented in this paper. The cluster structure of energy levels associated with a resonance was obtained here for a particular system and resonance. However, the

accompanying analysis is easily generalized to show that a similar energy level pattern should apply for other systems (including those with more than two degrees of freedom) and other resonances, provided that the relevant portion of the Hamiltonian can be cast into Chirikov form, that the parameter being varied is the detuning of the zero-order frequencies and that the resonance interaction is sufficiently weak. We have, in fact verified that the pattern of levels produced by the 2:1 resonance of our system is similar to that described in this paper. There are, of course, factors that may lead to slight variations in the observed patterns, in certain cases. For example, if the anharmonicity of the oscillators (which is proportional to ω_1') is positive, the clusters will be inverted, with the nonresonant levels of each cluster lying above the resonant energies.

Looking beyond the case treated in this paper, it should be recognized that the specific pattern associated with a resonance will certainly depend on the parameter being varied in the Hamiltonian. If that parameter is not the detuning between the zero-order frequencies, the resulting pattern will differ from that described in this paper. In addition, the pattern will differ significantly from that described here if the resonance interaction is too strong. In our calculations, the different resonances and clusters were well separated because the interaction between the zero-order oscillators was chosen to be rather weak (the value of ρ was chosen to be small). In systems with stronger interaction, these may overlap more. The resulting avoided crossings may be expected to cause extensive distortion of the cluster structure discussed in this paper. In some cases, the interaction between curves may signify quantum effects, such as tunneling; in others, they may signify classical effects such as the onset of chaos or the formation of secondary and higher-order resonances. Investigations of the energy curves in such more general cases are in progress.

APPENDIX: ENERGY LEVELS OF THE RESONANCE HAMILTONIAN

We examine the solutions of the problem

$$\left[-\frac{\hbar^2}{2}\omega_1'\frac{\partial^2}{\partial\phi_2^2}-\frac{i\hbar}{2}(\omega_1-\omega_2)\frac{\partial}{\partial\phi_2}+2V_R\cos\phi_2\right]\Psi(\phi_2)$$
$$=E\Psi(\phi_2), \tag{A1}$$

subject to the boundary conditions $\Psi(0)=\Psi(2\pi)$. In particular, we are concerned with the behavior of the energy levels as the parameter ω_2 is varied. To facilitate the analysis, we eliminate the linear term in $\partial/\partial\phi_2$ by, in effect, transforming to the new action $I_2+(\omega_1-\omega_2)/2\omega_1'$ of Eq. (14b) by the substitution $\Psi(\phi_2)=F(\phi_2)e^{i\gamma\phi_2}$, where $\gamma=-(\omega_1-\omega_2)/(2\hbar\omega_1')$. Then $F(\phi_2)$ satisfies the Mathieu equation

$$-\frac{h^2}{2}\omega_1'F''+[2V_R\cos\phi_2-E_{HR}]F=0, \tag{A2}$$

where

$$E_{HR}=E+\frac{(\omega_1-\omega_2)^2}{8\omega_1'}=E+E'. \tag{A3}$$

The condition $\Psi(0)=\Psi(2\pi)$ implies that the desired solutions of Eq. (A1) satisfy the nonstandard boundary conditions $F(0)=F(2\pi)e^{(2\pi i\gamma)}$.

We now consider two extreme cases in which it is simple to obtain approximate solutions of Eq. (A2); approximate solutions in more general situations can be found by semiclassical techniques.[11,15–17,23,28,47]

1. States deep within the resonance

For a state with energy sufficiently near the top of the inverted cosine barrier ($E_{HR}\sim 2V_R$), the wave function Ψ is small at $\phi_2=0$ and 2π, causing F to likewise become small at 0 and 2π. E_{HR} therefore become ordinary hindered rotor energy eigenvalues for standard boundary conditions at $\phi_2=0$ and 2π. Since Eq. (A2) shows such eigenvalues to be independent of ω_2, the energies E depend on ω_2 only via the term E' in Eq. (A3), which describes a common functional dependence for all levels deep in the well. This implies that such levels run parallel to each other and do not cross.

2. States well outside the resonance

For a state with energy far beyond the potential barrier ($E_{HR}\ll -2V_R$), we may, as a zeroth-order approximation, neglect the cosine term in Eq. (A1). The solution of this equation is of the form $A\exp(ik\phi_2)$ with

$$\frac{\hbar^2}{2}\omega_1'k^2-E_{HR}=0. \tag{A4}$$

The boundary conditions imposed on F lead to the requirement that $e^{2\pi i(k+\gamma)}=1$, which means that $(k+\gamma)=m$, where m is any positive or negative integer. Symmetry considerations, however, show that m should be restricted to have the same parity as n. Substituting $k=m-\gamma$ into Eq. (A4), we get

$$E_m=\frac{\hbar^2}{2}\omega_1'm^2+\frac{\hbar}{2}(\omega_1-\omega_2)m$$

which, of course, agrees with the expression for zero-order energies contained in Eq. (18). When regarded as a function of ω_2, this expression describes the energy levels as an infinite web of straight lines with slopes $-m\hbar/2$ that may be positive or negative. Such levels intercept one another at the regularly spaced frequency intervals $\omega_2-\omega_1=\pm 2\hbar\omega_1'$, $\pm 4\hbar\omega_1'$, $\pm 6\hbar\omega_1'$,... . Restriction of m to the physically allowed values $-n$, $-n+2$,...,n produces patterns with a finite number of crossings such as those shown in Fig. 3(a). The crossings predicted by this zeroth order approximation become avoided crossings when the potential $2V_R\cos\phi_2$ is taken into account by degenerate perturbation theory.[22]

This analysis shows clearly that, for the hindered rotor model, the parallel energy curves correspond to resonant states, while the curves that undergo avoided crossings correspond to nonresonant states. It also suggests that the

same conclusions apply to the actual energy curves for our system (Fig. 2), which, as we have shown, are related to those of the hindered rotor.

[1] T. Uzer, Phys. Rep. **199**, 73 (1991).
[2] E. L. Sibert III, W. P. Reinhardt, and J. T. Hynes, J. Chem. Phys. **77**, 3583 (1982).
[3] E. L. Sibert III, J. T. Hynes, and W. P. Reinhardt, J. Chem. Phys. **81**, 1135 (1984).
[4] T. Uzer and J. T. Hynes, Chem. Phys. Lett. **113**, 483 (1985).
[5] J. S. Hutchinson, W. P. Reinhardt, and J. T. Hynes, J. Chem. Phys. **79**, 4247 (1983).
[6] J. S. Hutchinson, J. T. Hynes, and W. P. Reinhardt, J. Phys. Chem. **90**, 3528 (1986).
[7] B. V. Chirikov, Phys. Rep. **52**, 265 (1979); G. M. Zaslavski and B. V. Chirikov, Usp. Fiz. Nauk **105**, 3 (1972) [Sov. Phys. Usp. **14**, 549 (1972)].
[8] A. J. Lichtenberg and M. A. Lieberman, *Regular and Stochastic Motion* (Springer, New York, 1981).
[9] E. V. Shuryak, Zh. Eksp. Teor. Fiz. **71**, 2039 (1976) [Sov. Phys. JETP **44**, 1070 (1976)].
[10] K. G. Kay, J. Chem. Phys. **72**, 5955 (1980).
[11] E. L. Sibert, J. T. Hynes, and W. P. Reinhardt, J. Chem. Phys. **77**, 3595 (1982).
[12] R. T. Lawton and M. S. Child, Mol. Phys. **44**, 709 (1981).
[13] R. T. Lawton and M. S. Child, Mol. Phys. **37**, 1799 (1979).
[14] (a) M. E. Kellman, J. Chem. Phys. **83**, 3843 (1985); (b) L. Xiao and M. E. Kellman, *ibid.* **90**, 6086 (1990).
[15] G. A. Voth and R. A. Marcus, J. Chem. Phys. **82**, 4064 (1985).
[16] G. A. Voth, J. Phys. Chem. **90**, 3624 (1986).
[17] D. Farrelly and T. Uzer, J. Chem. Phys. **85**, 308 (1986).
[18] S. K. Gray and M. S. Child, Mol. Phys. **53**, 961 (1984).
[19] M. S. Child and L. O. Halonen, Adv. Chem. Phys. **57**, 1 (1984).
[20] R. A. Marcus, in *Horizons in Quantum Chemistry, Proceedings of the Third International Congress in Quantum Chemistry, Kyoto, 1979*, edited by K. Fukui and B. Pullman (Reidel, Dordrecht, 1980), p. 107; Ann. N. Y. Acad. Sci. **357**, 169 (1980); Faraday Discuss. Chem. Soc. **75**, 103 (1983).
[21] D. W. Noid, M. L. Koszykowski, M. Tabor, and R. A. Marcus, J. Chem. Phys. **72**, 6168 (1980); D. W. Noid, M. L. Koszykowski, and R. A. Marcus, Chem. Phys. Lett. **73**, 269 (1980).
[22] (a) R. Ramaswamy and R. A. Marcus, J. Chem. Phys. **74**, 1379 (1981); (b) **74**, 1385 (1981).
[23] A. M. Ozorio de Almeida, J. Phys. Chem. **88**, 6139 (1984).
[24] K. K. Lehmann, J. Chem. Phys. **79**, 1098 (1983).
[25] E. J. Heller, E. B. Stechel, and M. J. Davis, J. Chem. Phys. **73**, 4720 (1980).
[26] B. Eckhardt, Phys. Rep. **163**, 205 (1988).
[27] D. W. Noid, M. L. Koszykowski, and R. A. Marcus, J. Chem. Phys. **78**, 4018 (1983).
[28] T. Uzer, D. W. Noid, and R. A. Marcus, J. Chem. Phys. **79**, 4412 (1983).
[29] C. Jaffe, J. Chem. Phys. **85**, 2885 (1986); C. Jaffe and M. Watanabe, *ibid.* **86**, 4499 (1987).
[30] S. Graffi, T. Paul, and H. J. Silverstone, Phys. Rev. Lett. **59**, 255 (1987); Phys. Rev. A **37**, 2214 (1988).
[31] M. V. Berry, in *Chaotic Behavior in Quantum Systems*, edited by G. Casati (Plenum, New York, 1985).
[32] L. E. Reichl and W. A. Lin, Phys. Rev. A **33**, 3598 (1986); W. A. Lin and L. E. Reichl, *ibid.* **36**, 5099 (1987); **37**, 3972 (1988).
[33] P. Gaspard, S. A. Rice, H. J. Mikeska, and K. Nakamura, Phys. Rev. A **42**, 4015 (1990).
[34] T. Takami and H. Hasegawa, Phys. Rev. Lett. **68**, 419 (1992).
[35] M. Wilkinson, J. Phys. A **22**, 2795 (1989).
[36] J. Goldberg and W. Schweizer, J. Phys. A **24**, 2785 (1991).
[37] C. Cohen-Tannoudji, B. Diu, and F. Laloe, *Quantum Mechanics* (Wiley, New York, 1977), Vol. 1, Chap. 4, p. 408.
[38] M. J. Davis and E. J. Heller, J. Chem. Phys. **75**, 246 (1981).
[39] B. Ramachandran and K. G. Kay, Phys. Rev. A **41**, 1757 (1990).
[40] D. Farrelly and W. P. Reinhardt, J. Chem. Phys. **78**, 606 (1983).
[41] W. P. Reinhardt, in *Chaotic Behavior in Quantum Systems*, edited by G. Casati (Plenum, New York, 1985).
[42] E. J. Heller, Faraday Discuss. Chem. Soc. **75**, 141 (1983).
[43] M. Wilkinson, J. Phys. A **20**, 635 (1987).
[44] T. Takami, Phys. Rev. Lett. **68**, 3371 (1992).
[45] C. Jaffe and P. Brumer, J. Chem. Phys. **73**, 5646 (1980).
[46] D. W. Oxtoby and S. A. Rice, J. Chem. Phys. **65**, 1676 (1976).
[47] C. Jaffe and W. P. Reinhardt, J. Chem. Phys. **77**, 5191 (1982).
[48] M. J. Davis, J. Phys. Chem. **92**, 3124 (1988).
[49] M. E. Kellman and L. Xiao, Chem. Phys. Lett. **162**, 486 (1989); J. Chem. Phys. **93**, 5821 (1990).
[50] E. A. Solov'ev, Zh. Eksp. Teor. Fiz. **75**, 1261 (1978) [Sov. Phys. JETP **48**, 625 (1978)].
[51] R. T. Skodje, F. Borondo, and W. P. Reinhardt, J. Chem. Phys. **82**, 4611 (1985).
[52] B. R. Johnson, J. Chem. Phys. **83**, 1204 (1985).
[53] C. W. Patterson, J. Chem. Phys. **83**, 4618 (1985).
[54] T. P. Grozdanov, S. Saini, and H. S. Taylor, Phys. Rev. A **33**, 55 (1986); J. Chem. Phys. **84**, 3243 (1986).
[55] For reviews of the adiabatic switching method, see R. T. Skodje and J. R. Cary, Comput. Phys. Rep. **8**, 221 (1988); W. P. Reinhardt, Adv. Chem. Phys. **73**, 925 (1989).
[56] S.-W. Cho and K. G. Kay, J. Phys. Chem. **92**, 602 (1988).
[57] M. V. Berry, J. Phys. A **17**, 1225 (1984).